Fibers and Polymers (2024) 25:661–672
https://doi.org/10.1007/s12221-023-00465-5

Online ISSN 1875-0052
Print ISSN 1229-9197

REGULAR ARTICLE

Investigating the Influence of Stacking Sequences on the Physical and Mechanical Characteristics of Coconut Coir Fiber-Reinforced Unsaturated Polyester Composites

M. R. M. Asyraf[1,2] · Agusril Syamsir[3,4] · A. B. M. Supian[3] · M. A. F. M. Zaki[4] · K. Z. Hazrati[5] · W. Ashraf[6] · Vivi Anggraini[7] · Emrah Madenci[8] · Yasin Onuralp Özkılıç[8] · Ceyhun Aksoylu[9]

Received: 9 August 2023 / Revised: 10 December 2023 / Accepted: 24 December 2023 / Published online: 10 January 2024

Abstract

The coconut fruit is cultivated for fruit in tropical countries, whereas its husk and shell are a potential source of natural fiber, which is mostly disposed of as waste material. There is an increasing trend in research and innovation to replace synthetic fiber with natural fiber to reduce the environmental carbon footprint. However, using natural fiber in polymer composite is challenging because of the lower mechanical strength and hydrophilic nature of the natural fiber. The literature reported on mechanical and moisture resistance properties of coir fiber polymer composite with different fiber orientations is very limited. Thus, this research aims to evaluate the mechanical properties (flexural and impact) and moisture resistance properties of the coir fiber reinforced composite. The fiber ware stacked with three different fiber orientations, namely 0°/0°/0°, 0°/90°/0° and 0°/+45°/0°. The composite was fabricated with the hand lay-up technique. The overall results indicated that the composite specimens with the orientation of 0°/0°/0° indicated the best flexural properties and water penetration resistance in the composite. The stacking sequence of 0°/+45°/0° gave the best impact properties. However, at this orientation, it gave the lowest water resistance among the studied configurations.

Keywords Coconut coir fiber · Stacking sequence · Thermoset · Water absorption · Mechanical properties

✉ M. R. M. Asyraf
muhammadasyraf.mr@utm.my

✉ Agusril Syamsir
agusril@uniten.edu.my

A. B. M. Supian
mohd.supian@uniten.edu.my

K. Z. Hazrati
hazrati88@gmail.com

W. Ashraf
shwaqas88@gmail.com

Vivi Anggraini
vivi.anggraini@monash.edu

Emrah Madenci
emadenci@erbakan.edu.tr

Yasin Onuralp Özkılıç
yozkilic@erbakan.edu.tr

Ceyhun Aksoylu
caksoylu@ktun.edu.tr

[1] Engineering Design Research Group (EDRG), Faculty of Mechanical Engineering, Universiti Teknologi Malaysia, 81310 Johor Bahru, Johor, Malaysia

[2] Centre for Advanced Composite Materials (CACM), Universiti Teknologi Malaysia, 81310 Johor Bahru, Johor, Malaysia

[3] Institute of Energy Infrastructure, Universiti Tenaga Nasional, Jalan IKRAM-UNITEN, 43000 Kajang, Selangor, Malaysia

[4] Civil Engineering Department, College of Engineering, Universiti Tenaga Nasional, Jalan IKRAM-UNITEN, 43000 Kajang, Selangor, Malaysia

[5] German Malaysian Institute, Jalan Ilmiah, Taman Universiti, 43000 Kajang, Selangor, Malaysia

[6] Department of Textile Engineering, National Textile University, Faisalabad 37610, Pakistan

[7] Civil Engineering Department, School of Engineering, Monash University Malaysia, Jalan Lagoon Selatan, Bandar Sunway, 47500 Subang Jaya, Selangor, Malaysia

[8] Department of Civil Engineering, Necmettin Erbakan University, 42090 Konya, Turkey

[9] Department of Civil Engineering, Konya Technical University, 42090 Konya, Turkey

1 Introduction

Composite materials play a pivotal role in advancing manufacturing processes, aiming to uphold quality standards while reducing material weight, especially in industries, such as aviation, automotive, aerospace, sports goods, and marine fields [1, 2]. The continual improvements in these sectors pose a challenge to producing composites with enhanced physical and mechanical properties [3, 4]. Natural fiber-reinforced polymer composites have garnered attention due to their potential to deliver improved mechanical characteristics, rendering them promising in practical applications [5–7]. The rising environmental consciousness has led to the development of eco-friendly materials, notably utilizing natural fibers, such as plants and wood, in place of conventional glass fibers across various applications [8–10]. The appeal of natural fibers lies in their renewability, biodegradability, cost-effectiveness, and ready availability. Integrating fibers effectively into structural designs enhances the mechanical strength of biocomposites [11–13].

Natural fibers derived from coconut coir [14], sisal [15], bamboo [16], banana [17], rice husk and straw [18, 19], kenaf [20], pineapple leaf [21], and jute [22] offer an opportunity to reduce composite density and cost while retaining strength. Historically used in a wide array of products, natural fibers, especially in recent times, have emerged as substitutes for traditional glass and carbon fibers in composite materials. The characteristics of these composites depend on factors like fiber–matrix adhesion, fiber length, loading, treatment, and matrix dispersion [23–25]. Tensile [26], flexural [27], and impact strength [28] are some of the mechanical properties that have been studied. Natural fibers are being used as alternatives in many fields, such as construction, aircraft, medicine, and electronics manufacturing [29], because they are strong, resist to rusting, are stiff, are lightweight, and not toxic [30, 31]. Research by Arun et al. [32] underscores how polymer composite materials can amalgamate polymer advantages with reinforced phase strength, establishing them as a widely used, expanding class of materials.

Coconut coir (*Cocos nucifera*), a robust lignocellulosic fiber derived from coconut fruit mesocarp, is extensively cultivated in tropical regions like Thailand, India, and Sri Lanka [33, 34]. Coir fibers possess a high lignin content, endowing them with strength, weather resistance, waterproofing, and chemical adaptability. Their notable elongation at break allows further stretching without fracturing. Literature extensively documents the structural, morphological, mechanical, and thermal characteristics of coir fibers [34, 35], as evident in Table 1 showcasing the chemical composition of coir fibers.

Table 1 Chemical composition of coconut coir fiber [36]

Components	Contents (%)
Cellulose	43.4
Hemicellulose	0.25
Lignin	45.8

Coconut coir fibers exhibit unique mechanical properties, making them promising reinforcements for polymer composites. Studies by Abdul Khalil et al. [37] highlight their impressive tensile strength, enhancing composite structural integrity. Additionally, the durability of coir fibers and its lightweight nature contribute significantly to the overall strength-to-weight ratio of the polymer composites [38]. Studies, like those by Munde et al. [39], emphasize that low fiber loading in coir-PP composites increases energy absorption due to higher damping characteristics at higher resin concentrations. Recent investigations and manufacturing applications of coir fiber-reinforced polymer composites, alongside other natural fibers, are detailed in Table 2, exemplifying their utilization and manufacturing processes.

The utilization of coconut coir fibers, a byproduct of coconut husks, has gained recognition for strengthening polymer composites, primarily due to their significant tensile strength [41, 42]. Research by Abdul Khalil et al. [37, 43] emphasizes natural fibres' tensile strength, positioning them as reinforcing agents. Favorable integration of coir fibers with unsaturated polyester matrices for composite laminates stems from their high tensile strength. However, a comprehensive analysis of their mechanical and physical properties concerning compatibility with unsaturated polyester resin remains essential. Table 3 summarizes the mechanical and physical properties of coconut coir fibers and unsaturated polyester, highlighting their respective characteristics.

Despite extensive research on diverse fiber composites, insufficient attention has been given to coconut coir fiber-reinforced unsaturated polyester composites [47, 48]. This gap is intriguing considering the existing knowledge of manufacturing techniques and the mechanical properties of various fiber composites. Addressing this lack of study is critical, given the rising demand for sustainable and high-performance materials. Therefore, this research aims to comprehensively investigate coconut coir fibre's potential as reinforcement in unsaturated polyester composites. Understanding the relationship between the mechanical properties and water absorption characteristics of these composites is vital for their real-world applicability. By bridging this knowledge gap, this study aims to significantly contribute to the development of environmentally friendly materials exhibiting superior performance.

Table 2 Current progress of coir fiber and other natural fibers in composite products and applications [40]

Fibre reinforcement	Matrix/Binder Material	Application	Manufacturing techniques
Coir	PP, epoxy resin, PE	Automobile structural components, building boards, roofing sheets, insulation boards	Extrusion, injection molding
Ramie	PP, Polyolefin, PLA	Bulletproof vests, socket prosthesis, civil. Window/door frames, automative structure	Extrusion with injection molding
Kenaf	PLA, PP, epoxy resin	Tooling, bearings, automotive parts	Compression molding, pultrusion
Flax	PP, polyester, epoxy	Structural, textile	Compression molding, RTM, spray/hand lay-up vacuum infusion
Jute	Polyester, PP	Ropes, roofing, door panels	Hand lay-up, compression/injection molding
Sisal	PP, PS, epoxy resin	Tooling, automotive	Hand layup, compression molding
Hemp	PE, PP, PU	Furniture, automotive	RTM, compression molding

Table 3 Mechanical and physical properties of coconut coir fiber and unsaturated polyester [44–46]

Properties	Coconut coir fiber	Unsaturated polyester
Density (g/cm^3)	1.15–1.46	1.025
Tensile strength (MPa)	131–220	44.40
Elastic modulus (GPa)	4–6	3.54
Elongation at break (%)	15–40	2.15

2 Materials and Methods

2.1 Materials

Fibers from coconut coir (*Cocos nucifera*) were extracted in Dungun, Terengganu, Malaysia. CCP Composites Resins Malaysia Sdn. Bhd. The matrix material, an unsaturated polyester resin of RTM grade, was carefully chosen for its favorable viscosity and reactivity. This resin, with a density of 1.025 g/cm^3, not only influences the overall weight of the resulting composite but also ensures compatibility with the coir fibers. In order to start the curing process, the application of methyl-ethyl ketone peroxide (MEKP), more precisely the Butanox-M50 version, was used. The MEKP compound functioned as the catalyst, facilitating the polymerization process of the liquid resin, resulting in the formation of a composite laminate. The selection of Butanox-M50 MEKP aids in providing the polymer matrix to be optimal in both reactivity and stability. The careful methodology used in the selection and processing of materials establishes the foundation for a thorough examination of the mechanical and water absorption characteristics of the unsaturated polyester composites reinforced with coconut coir fibers.

2.2 Fabrication of Composite Samples

The coconut coir reinforced polymer composites were developed using a hand-layup method with a 17:100 ratio of coir fiber to unsaturated polyester resin. The coir fiber was not given any treatment during the investigation. First, a silicone release agent was sprayed into the mold to eliminate the possibility of the composites sticking to the mold. 1 g of MEKP, which served as a hardener, was thoroughly incorporated into the unsaturated polyester resin. Three layers of coir fiber were piled in the mold before the resin was poured over them. The sample was allowed to cure for a week. As illustrated in Fig. 1, three different stacking sequences were used to fabricate composite laminates: 0°/0°/0°, 0°/90°/0°, and 0°/+45°/0° as shown in Fig. 1. The final thickness of the produced samples approximately 7 to 8 mm. Following the guidelines in ASTM 570 (Water Absorption Test), ASTM 6272 (Four-Point Flexural Test), and ASTM D6110 (Charpy Impact Test) standards, the composite laminates were divided into numerous dimensions of coupons once they had cured. Six samples were created for each composite configuration to investigate each sample's water absorption, flexural characteristics, and impact properties. Figure 2 shows the overall composite production procedure.

2.3 Density Test

A densimeter (Mettler Toledo (M) Sdn. Bhd, Selangor, Malaysia) was used in the determination of the density of acquired three stacking sequences of coconut coir fiber reinforced unsaturated polyester composites. The samples were dried for 7 days. Afterward, the computation of the initial dry matter of each composite was accomplished. The coir/UPE composites samples were weighed (m) before immersing hybrid composites into the liquid of volume (V) and the density denoted as (ρ), was calculated from Eq. (1). The

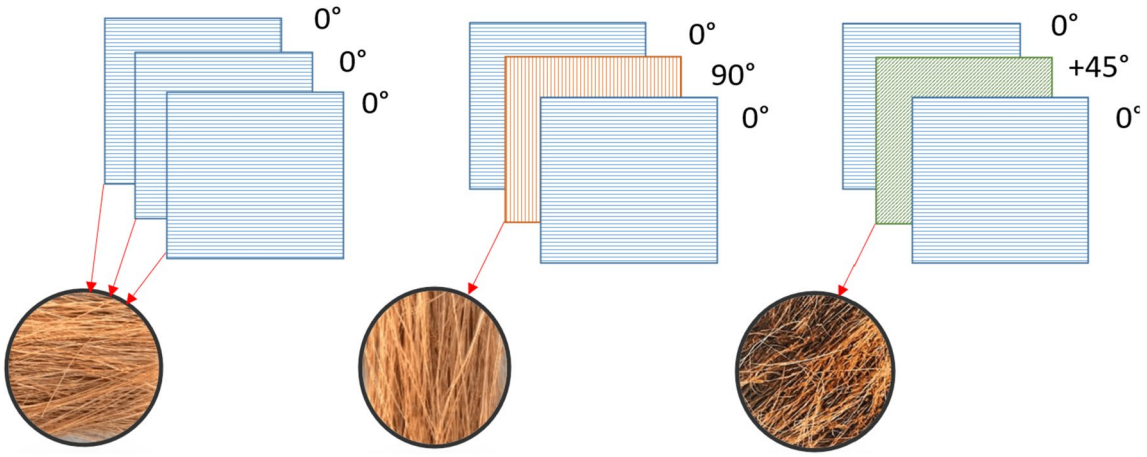

Fig. 1 Stacking sequences of coir fibers reinforced UPE composites

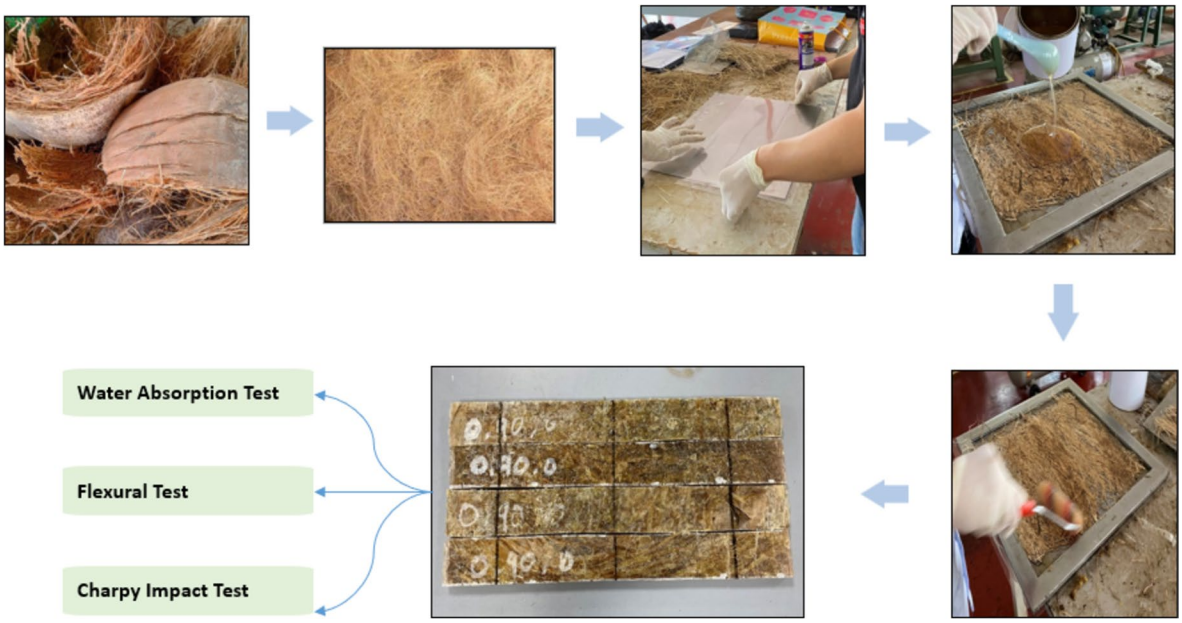

Fig. 2 Fabrication process of coir fibers reinforced UPE composites

samples were set with size of 4 cm × 6 cm × 0.8 cm. Each test was carried out 6 times.

$$\rho = \frac{M}{V}. \tag{1}$$

2.4 Water Absorption Test

An investigation on water absorption was carried out using the methodology outlined in ASTM D 570. The samples were dried for 24 h at a temperature of 50 °C, and to stabilize their weight, the dried samples were cooled in a desiccator. The samples were weighed and immediately soaked in distilled water at room temperature. After being cleaned off with a clean piece of cloth, the samples of the wet film were reweighed. The initial and final mass were determined, and Eq. (2) was used to calculate the water absorption (%).

$$\text{Water absorption}(\%) = \frac{M_\text{f} - M_\text{i}}{M_\text{i}} \times 100, \tag{2}$$

where M_i is the initial mass of the dried sample, M_f is the final mass of the sample after water absorption.

2.5 Moisture Content and Thickness Swelling Test

Moisture content and thickness swelling are pivotal parameters used to gage a material's interaction with moisture,

particularly in composite materials like fiber-reinforced polymers. Moisture content assessment serves to quantify the quantity of water absorbed relative to the material's dry weight or volume, offering insights into its stability and durability in varying environmental conditions. The moisture content test is performed based on ASTM D4442-92 standards. The procedure entails precisely weighing dry samples at first, then thoroughly drying them to remove moisture. The final weight post-drying facilitates the calculation of moisture content as a percentage (Eq. 3).

$$\text{Moisture Content } (\%) = \left(\frac{\text{Wet weight} - \text{Dry weight}}{\text{Dry Weight}}\right) \times 100. \tag{3}$$

Conversely, thickness swelling evaluation determines a material's expansion or swelling when exposed to moisture, which is crucial for assessing dimensional changes. This test requires initial thickness measurements, and immersion of samples in water for a designated period, followed by re-measuring post-soaking thickness. Test method based on ASTM D1037 measures the thickness swelling of wood-based panels or composites after being subjected to water immersion. The percentage increase in thickness is calculated to ascertain the extent of swelling. Both tests aid in material selection, quality control, and assessing a material's suitability in environments with moisture exposure, providing critical insights into dimensional stability and overall durability. Thickness swelling (%) is calculated as follows (Eq. 4):

$$\text{Thickness Swelling } (\%) = \left(\frac{\text{Final Thickness} - \text{Initial Thickness}}{\text{Initial Thickness}}\right) \times 100. \tag{4}$$

Subsequently, the moisture content and thickness swelling measurements are crucial in assessing the performance and suitability of materials in environments where exposure to moisture is expected. Both parameters help in determining a material's dimensional stability, durability, and overall behavior when used in real-world conditions where water contact or humidity are concerns. These tests aid in material selection, quality control, and ensuring the reliability of materials in various applications.

2.6 Four-Point Flexural Test

The ultimate flexural strength was assessed using the four-point flexural test (Fig. 3) at room temperature at the Material Laboratory, Universiti Tenaga Nasional, Malaysia. Based on the ASTM D6272, an international testing standard for the four-point bending test, the cross-head speed of 3.29 mm/min was selected. According to ASTM D6272 requirements, the span-to-depth support and span-to-depth shear ratios were around 28 and 10.45, respectively, sufficient to minimize shear effects. The edges of the loading channels were rounded with a 2.5 mm radius. Each flexural specimen was supported by steel rollers with a diameter of 12.7 mm over a 280 mm clear span. A strain gage positioned in the middle of the specimen was used to measure the flexural strength throughout the test. The four-point flexural tests were performed three times, the average results were taken, and then the results were recorded for evaluation and discussion.

The below illustrates the ultimate flexural strength and flexural strain of a rectangular sample with a loading span of one-third the ratio of the support loading span. Equations (5) to (7) shows the calculations of flexural stress, strain and modulus respectively.

$$\sigma = \frac{3P(L - L_i)}{2bd^2} \tag{5}$$

$$\varepsilon = \frac{6(L - L_i)d\Delta}{4a^3 - 3aL^2} \tag{6}$$

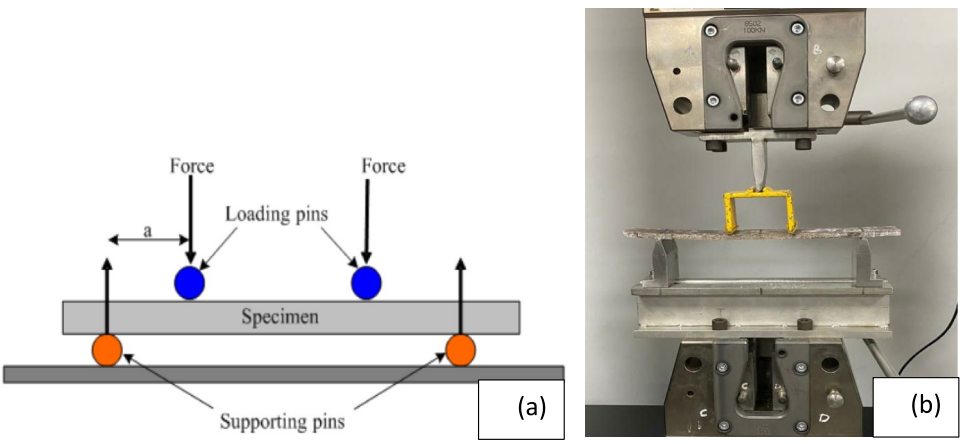

Fig. 3 Composite specimen subjected to four-point flexural test: **a** schematic diagram and **b** actual test conducted using a universal test machine

$$E = \frac{\sigma}{\varepsilon}. \tag{7}$$

where P is the load in (N), σ is stress in the outer fiber in (MPa), L_i is the loading span in (mm), L is the support span in (mm), a is the distance from the support to the nearest loading point in (mm), b is the specimen width in (mm), d is the specimen thickness in (mm), Δ is the midspan deflection in (mm), and E is flexural modulus (GPa) using Hooke's law equation.

2.7 Charpy Impact Test

At room temperature, the Charpy impact test was carried out in the Material Laboratory of the Universiti Tenaga Nasional, Malaysia, to evaluate composites' impact strength and ability to absorb energy. Zwick Roell Pendulum Impact Testers used for Charpy impact test following ASTM D6110. The specimens were 63.5 mm × 12.7 mm in size. An impact test was carried out to investigate the composite material's mechanical properties in terms of its ability to withstand high-speed loading. Results were obtained from an average of 5 tested specimens for each loading.

3 Results and discussion

3.1 Density

The density values of unsaturated polyester composites reinforced with coconut coir fibers when stacked in three different ways are 0°/0°/0°, 0°/90°/0°, and 0°/ + 45°/0°. These values show clear differences. The 0°/0°/0° composites exhibited the highest density at 0.684 g/cm^3, followed by the 0°/90°/0° configuration at 0.564 g/cm^3, and the 0°/ + 45°/0° configuration at 0.451 g/cm^3. The transition from 0° fiber orientation to 90° and + 45° orientations appears to decrease the composite's density, presumably due to the alteration in fiber orientations creating discontinuities between fiber stacks, consequently reducing the mass of fibers per unit volume. Lower density values suggest a lighter composite material, indicating that stacking sequence and fiber orientation significantly influence the composite's physical properties (see Table 4).

In the parallel fiber stacking sequence (0°/0°/0°), the coconut coir fibers are lined up parallel to each other. This makes the arrangement denser and more tightly packed, which increases the overall density of the material. The perpendicular fiber sequence (0°/90°/0°), where fibers are aligned at a precise right angle of 90 degrees to one another, although not as dense as the parallel sequence, still leads to a relatively dense structure [49]. On the contrary, the off-axis fiber sequence (0°/ + 45°/0°) positions fibers at a 45-degree angle, creating more voids within the composite, resulting in reduced overall density compared to other sequences [50].

Table 4 Density of coconut coir fiber-reinforced unsaturated polyester composites with various stacking sequences

Sample fiber orientation	Density (g/cm^3)
0°/0°/0°	0.684
0°/90°/0°	0.564
0°/ + 45°/0°	0.451

The positioning and alignment of the reinforcing fibers in a composite material affect its density. Parallel or tightly aligned fibers tend to lead to higher densities, whereas more randomly oriented or off-axis fibers tend to result in lower densities [51, 52]. Understanding this relationship among fiber orientation, stacking sequence, and resultant composite density is crucial in tailoring composite materials for specific applications while balancing variables, such as strength, stiffness, and weight [53]. Therefore, these density findings will be integrated with water absorption and mechanical characteristics investigations to optimize the performance of these composites for diverse engineering applications.

3.2 Water Absorption Properties

Biocomposites are usually experience hydrophilic condition, where they are sensitive toward water molecules due to its lignocellulosic fiber sources [54]. In this case, water absorption behavior plays vital role in determining the properties of the composites and should be prepared for this work. The experimental work on water absorption characteristics took place to evaluate the physical ability of a material to absorbed water in certain time and conditions. Generally, the physical properties of moisture diffusion are governed by several aspects, such as humidity, fiber volume fraction, temperature, number of voids, and viscosity of matrix [55, 56]. In general, the adhesion behavior of fiber with the matrix was due to reduced water absorption [57, 58]. Additionally, the high water uptake of natural fiber composites is due to the presence of amorphous substances, such as hemicellulose, lignin, wax, and structurally integrated water molecules [25, 59]. For this test, Fig. 4 illustrates the water absorption properties for various stacking sequences of coconut coir fiber reinforced unsaturated polyester composite (CCFRUPC).

The highest water uptake of CCFRUPC after 360 h was 35.6% (0°/ + 45°/0°), then trailed by 19.2% (0°/90°/0°) and 16.8% (0°/0°/0°). This phenomenon happened due to the CCFRUPC with 0°/ + 45°/0° sequence was more amorphous and structurally integrated with water molecules in its composition. The 0°/90°/0° and 0°/0°/0° CCFRUPC have almost same performance and permit better water resistance than 0°/ + 45°/0° due to probably less air voids in the composite.

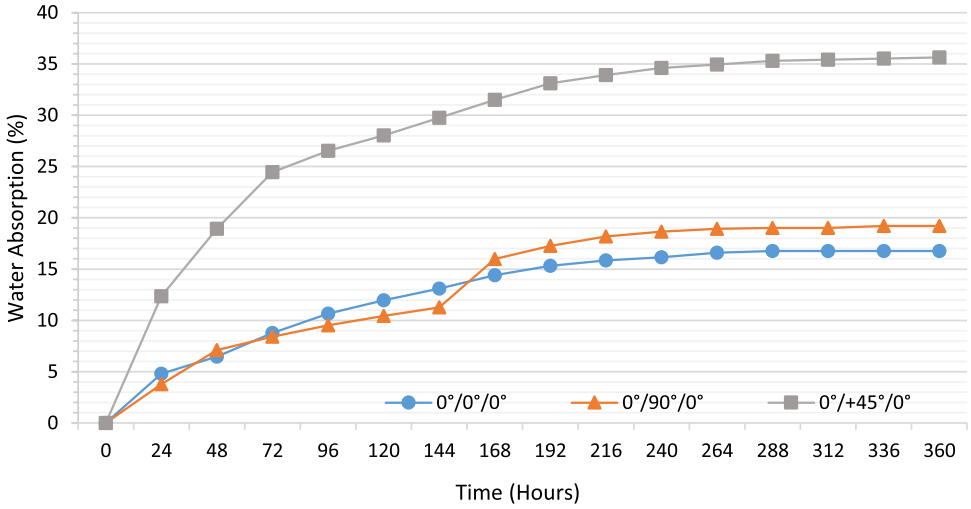

Fig. 4 Water absorption of CCFRUPC with various stacking sequences

According to Remirez et al. [60] and Jumaidin et al. [61], the lower water uptake in biocomposites was due to better interfaces adhesion between fibers/matrix which lesser voids and provide better resistance toward water molecule penetration. Other than that, the results displayed that water uptake was higher in the early period and start to be reduced as the longer immersion time at 168 h. This observation was because of water molecules beginning to enter the capillaries of composites and causing the fiber to swell and create more air cavities [62, 63]. This factor causes water to be trapped in the void and increases composite weight [64]. The cavities would induce to micro-crack in the thermosetting polyester matrix. Occurrence of micro-crack would create a large surface area at the interface between the fibers and the matrix and resulting higher water penetration toward the composite structure.

4 Moisture Content (MC) and Thickness Swelling Analysis

The investigation focused on assessing the moisture content and thickness swelling of coir fiber-reinforced polymer composites with three different fiber orientations: 0°/0°/0°, 0°/90°/0°, and 0°/+45°/0°. The moisture content and thickness swelling were crucial parameters measured during the experimental analysis, offering insights into the composite's resistance to moisture and dimensional changes under different orientations. The investigation involved assessing the moisture content and swelling of various coir fiber orientations incorporated into polymer composites. The collected data shown in Table 5 demonstrated notable differences among the tested samples.

The data obtained revealed varying moisture content among the different fiber orientations. The composite specimens with a stacking sequence of 0°/0°/0° exhibited the lowest moisture content, recorded at 2.1%. This orientation demonstrated superior resistance to moisture penetration, suggesting a more effective barrier against water absorption. The 0°/+45°/0° stacking sequence showcased the highest moisture content among the studied configurations, reaching 3.5%. This orientation exhibited increased vulnerability to moisture, indicating a higher propensity for water absorption compared to the 0°/0°/0° and 0°/90°/0° orientations. The 0°/90°/0° stacking sequence recorded a moisture content of 2.8%, indicating moderate resistance to moisture absorption. Overall, the moisture content data highlighted the significant influence of fiber orientation on the composite's ability to resist water penetration, with 0°, 0°, and 0° demonstrating the most favorable moisture resistance.

Table 5 Analysis moisture content and thickness swelling data

Sample fiber orientation	Moisture content (%)	Thickness swelling (%)
0°/0°/0°	2.1	1.5
0°/90°/0°	3.5	2.8
0°/+45°/0°	2.8	2.1

The thickness swelling data also showcased notable differences across the tested orientations. The 0°/0°/0° stacking sequence exhibited minimal thickness swelling, recorded at 1.5%. This orientation demonstrated remarkable dimensional stability when subjected to moisture, experiencing minimal changes in thickness. In contrast, the 0°/+45°/0° configuration displayed the highest thickness swelling among the tested sequences, reaching 2.8%. This orientation exhibited increased susceptibility to dimensional changes when exposed to moisture, resulting in greater swelling compared to the 0°/0°/0° and 0°/90°/0° orientations. The 0°/90°/0° stacking sequence showcased moderate thickness

swelling, recorded at 2.1%, indicating a moderate degree of dimensional change when exposed to moisture. The thickness swelling data emphasized the considerable impact of fiber orientation on the composite's dimensional stability under moisture exposure conditions, with the 0°/0°/0° configuration demonstrating the most favorable resistance to swelling.

Therefore, the moisture content and thickness swelling data underscored the critical role of fiber orientation in influencing the moisture resistance and dimensional stability of coir fiber-reinforced polymer composites. The 0°/0°/0° orientation exhibited superior performance in both moisture resistance and dimensional stability, making it a promising configuration for applications requiring high resistance to moisture absorption and minimal dimensional changes. Conversely, the 0°/ + 45°/0° orientation displayed higher susceptibility to moisture, leading to increased moisture content and thickness swelling. The findings highlighted the significance of selecting appropriate fiber orientations to optimize the composite's performance in resisting moisture and maintaining dimensional stability.

4.1 Flexural Properties

Flexural strength and modulus are critical mechanical properties that determine a material's ability to withstand bending or deformation when subjected to external loads. In our study, these properties were investigated across different stacking sequences (0°/0°/0°, 0°/90°/0°, and 0°/ + 45°/0°) of CCFRUPC. The 0°/0°/0° sequence, characterized by parallel fiber alignment, exhibited the highest flexural strength (24.1 MPa) and modulus (8.65 GPa). This superior performance can be attributed to the parallel orientation of fibers, which enables effective stress transmission along the length of the fibers during loading. When stress is applied parallel to the fiber orientation, the fibers efficiently bear the load, resulting in enhanced flexural properties. Likewise, the 0°/90°/0° and 0°/ + 45°/0° sequences showcased a significant decrease in flexural strength and modulus. The 0°/90°/0° sequence, with fibers arranged perpendicular to each other in the middle layer, recorded a reduced flexural strength of 11.98 MPa and a modulus of 5.32 GPa. The 0°/ + 45°/0° sequence, which used off-axis fibers at a 45-degree angle, showed even lower flexural strength (4.96 MPa) and modulus (1.71 GPa) (see Fig. 5).

The decline in flexural properties in configurations other than 0°/0°/0° suggests a notable lack of efficient stress transfer along the composite structure. When stress is applied perpendicular to or at off-axis angles to the fibers, the load transmission between layers becomes less effective [65, 66]. This phenomenon leads to a reduced ability of the composite to withstand bending forces, resulting in lower flexural strength and modulus [67, 68]. Hashim et al.'s research results [51] agree with what we saw. They stress that the lack of stress transfer, especially in patterns like 0°/90°/0° and 0°/ + 45°/0°, can weaken the structure of composites when loads are put on them. The misalignment or change in the orientation of fibers in these sequences contributes to a lack of continuity in load-bearing pathways, reducing the material's ability to resist deformation.

Therefore, this result confirms that the stacking sequence and fiber orientation significantly influence the flexural properties of CCFRUPC. Configurations like 0°/0°/0°, which favors parallel fiber alignment, have better flexural strength and modulus. Deviations from this arrangement, on the other hand, cause mechanical performance to be worse. Understanding these relationships is crucial for designing composite materials optimized for specific applications, balancing properties like strength, stiffness, and load-bearing capacity.

4.2 Impact and Energy Absorption Properties

The results of the impact properties of CCFRUPC, shown in Fig. 6, show how the three stacking sequences (0°/0°/0°, 0°/90°/0°, and 0°/ + 45°/0°) have different effects on the composites. These stacking patterns show different ways

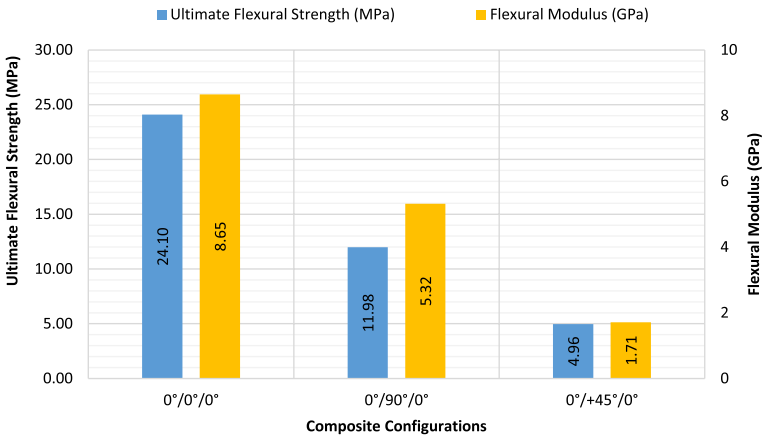

Fig. 5 Flexural strength and modulus of CCFRUPC with various stacking sequences

that the coir fibers are arranged in the composite structure, which changes how it reacts to impacts and how much energy it absorbs. The stacking sequence 0°/90°/0°, which looked like a sandwich with a 90° layer between two 0° layers, had the highest values for both energy absorbed (2.22 J) and impact strength (23.16 kJ/m2). This configuration displayed superior energy absorption capabilities, primarily due to its arrangement allowing for efficient load distribution and energy dissipation throughout the composite [69]. The 90° layer facilitates a better spread of impact forces, thus enhancing the material's ability to absorb and dissipate energy, resulting in improved impact strength.

Contrastingly, the 0°/0°/0° and 0°/+45°/0° configurations demonstrated lower energy absorption, mainly attributed to their orientations that restrict effective energy transfer and dissipation. These orientations led to localized stress concentrations, reducing the composite's ability to uniformly distribute the applied energy. As a consequence, these sequences exhibited surface failures, such as fiber breakage, delamination, and crack initiation, indicating limitations in their impact resistance. The fact that the impact properties changed when the layers were stacked in different ways shows how important fiber orientation is for how well CFRUP composites can absorb and release energy. The perpendicular arrangement in the 0°/90°/0° sequence made it much better at supporting weight and distributing energy, which made it more resistant to impact.

Besides, a comparative study conducted by Dress et al. [70], examining impact properties in woven sisal fiber-reinforced polyester composites (WSFRPC) with various orientations, corroborate these findings. Similar trends were observed, highlighting the advantageous impact properties of orientations resembling 0/90° compared to other angular configurations and affirming the importance of specific stacking sequences in governing impact resistance [71]. Furthermore, Fig. 6 shows how the impact strength and absorption properties change when coir fiber-reinforced UPE composites are stacked in different ways. Understanding how stacking configurations influence impact properties aid in tailoring these composites for applications where resilience against impact loads is crucial.

5 Analysis of Results from Density, Water Absorption, Flexural and Impact Properties due to the Effect of Fiber Orientations

The stacking sequences used in unsaturated polyester composites reinforced with coconut coir fibers—namely, 0°/0°/0°, 0°/90°/0°, and 0°/+45°/0°—have a big impact on how the composite material behaves as a whole. Density, a fundamental attribute, demonstrates a complex interdependence with fiber orientation and structural configuration. The 0°/0°/0° stacking configuration, characterized by parallel fibers, yields the highest density (0.684 g/cm^2), indicative of a highly compact and condensed arrangement. Conversely, the 0°/+45°/0° sequence, integrating off-axis fibers, results in the lowest density (0.451 g/cm^2), suggesting a less dense and more amorphous shape. The observed variations in density can be attributed to the formation of voids between fiber stacks due to orientation differences, influencing the mass of fibers within a given volume. Lower density, as seen in the 0°/+45°/0° stacking sequence, suggests a comparatively lighter composite material. This emphasizes the significant impact of layer arrangement and fiber orientation on the mechanical and physical properties of the composite material.

Beyond density, this study investigates the water absorption characteristics of these biocomposites, a crucial consideration due to their inherent hydrophilic nature. Results from the 360-h water uptake experiment indicate that the 0°/+45°/0° sequence exhibits the highest absorption rate at 35.6%. This is followed by the 0°/90°/0° sequence at 19.2% and the 0°/0°/0° sequence at 16.8%. The inclusion of an off-axis arrangement in the 0°/+45°/0° configuration increases

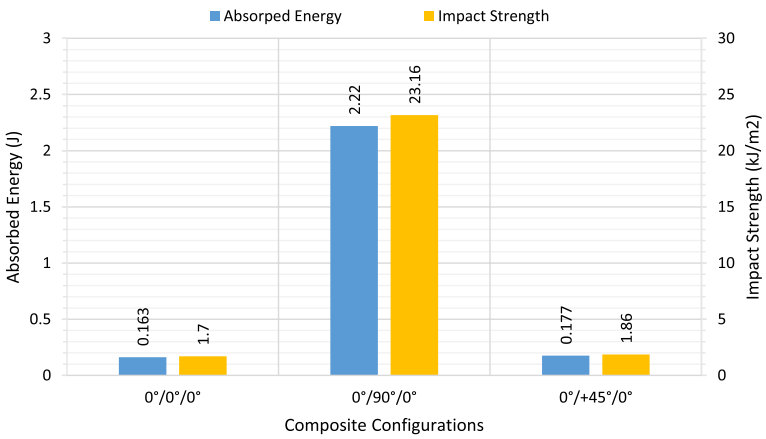

Fig. 6 Impact strength and absorption properties of various staking sequence of CCFRUPC

void presence, rendering it more amorphous and susceptible to water absorption. Conversely, enhanced adhesion in the 0°/90°/0° and 0°/0°/0° configurations decreases water absorption, emphasizing the influence of fiber–matrix interfaces on water repellency [41].

Looking at the flexural properties shows that the 0°/0°/0° sequence has the highest flexural strength (24.1 MPa) and modulus (8.65 GPa), which is because stress is easily transferred along the parallel fibers. On the other hand, the 0°/ + 45°/0° sequence has the lowest flexural strength (4.96 MPa) and modulus (1.71 GPa), which means that the change in fiber orientation has caused problems. Hashim et al. [51] also found out the both side of with 0° outer layers of coir composite allows principal loading direction aligned with the ply orientation. Subsequently, it caused degradation in the composite's structural integrity to resist the applied load. Impact and energy absorption characteristics consistently demonstrate that the 0°/90°/0° arrangement has the highest impact strength (2.22 J) and energy absorption capacity (23.16 kJ/m^2). These findings highlight the significance of fiber dispersion and alignment in governing impact resistance and energy absorption.

Comparatively, the parallel orientation (0°/0°/0°) often emerges as a preferable option due to its superior qualities in water absorption, flexural strength, modulus, impact strength, and energy absorption. Off-axis fibers (0°/ + 45°/0°) offer reduced density but encounter limitations in water absorption, flexural characteristics, and impact resistance. The sandwich configuration (0°/90°/0°) displays advantageous impact properties and energy absorption, making it suitable for applications prioritizing impact resistance. This result is consistent with finding made by Dress et al. [70] in which 0/90° orientation of woven sisal fiber reinforced polyester composite (WSFRPC) has better impact properties in comparison to orientations, such as 30°/60° and 30°/ − 45° of WSFRPC. Overall, these observations regarding the interaction between stacking sequences and composite properties offer crucial insights for enhancing performance across various engineering applications. They underscore the intricate connections among fiber orientation, stacking sequence, and resulting composite characteristics.

6 Conclusions

In this study, the effect of coir fiber orientation was evaluated on the flexural properties which impact performance and water resistance of the coir fiber reinforced polymer composite. The outer and the lower layers of the reinforcement were stacked with the same orientation in all composite specimens, but the middle layer was stacked with three different orientations. In conclusion, it is found that the fiber orientation had a significant effect on the overall flexural properties, impact strength, energy absorption, and moisture resistance of the coir fiber reinforced composite. The 0°/0°/0° and 0°/90°/0° exhibited the best moisture resistance compared to the 0°/45°/0°. Stacking all the fibers in the same direction of 0°/0°/0° exhibited the best flexural strength and modulus compared to other stacking orientations of the fiber. The stacking orientation of 0°/90°/0° showed the highest impact strength and energy absorption properties among all the studied configurations. Thus, this experimental investigation showed that 0°/90°/0°-oriented coir fiber in polymer composite could achieve greater impact strength and moisture resistance than stacked fiber in the same direction. However, in application areas of coir fiber polymer composite where structure requires higher flexural strength and stiffness, it would prefer to use the fiber in the same direction to achieve higher flexural strength and flexural modulus.

Acknowledgements The authors are grateful to acknowledge the IRMC Universiti Tenaga Nasional (UNITEN) and the Institute of Energy Infrastructure (IEI), UNITEN for the financial support provided through Dato' Low Tuck Kwong (DLTK) International Research Grant 2023, through Project No: 20238002DLTK. This research paper is also funded by Universiti Teknologi Malaysia (UTM) through the UTM Encouragement Research Grant (UTMER) project "Characterizations of Hybrid Kenaf Fibre/Fibreglass Meshes Reinforced Thermoplastic ABS Composites for Future Use in Aircraft Radome Applications", grant number: PY/2022/03758 — Q.J130000.3824.31J25. The authors are grateful to acknowledge UNITEN and UTM for the facilities and financial support throughout the preparation of the research article.

Data Availability The data used to support the findings of this study are included within the article.

Declarations

Conflict of Interest The authors declare that they have no conflict of interest.

References

1. K.Z. Hazrati, S.M. Sapuan, M.Y.M. Zuhri, R. Jumaidin, J. Mater. Res. Technol. **15**, 1342 (2021)
2. K. A. Azlan, M. R. Mansor, B. E. Mohamad, J. Nat. Fibre Polym. Compos. **2**, 1 (2023)
3. N. Saba, K. Abdan, N.A. Ibrahim, BioResources **10**, 4530 (2015)
4. R. Mohamed, N.M. Hapizi, M.N. Norizan, N. Khairunnisa, Polimery/Polymers **66**, 559 (2021)
5. C. Baley, Compos. Part A Appl. Sci. Manuf.. Part A Appl. Sci. Manuf. **33**, 939 (2002)
6. M.N. Salleh, R.S. Chen, M.H. Ab Ghani, F.H. Kasim, A. Sahrim, Appl. Mech. Mater.. Mech. Mater. **695**, 131 (2014)
7. N.H. Rosli, S.M. Sapuan, Z. Leman, R.A. Ilyas, J. Nat. Fibre Polym. Compos. **1**, 1 (2022)
8. N. Saba, M. Jawaid, O.Y. Alothman, M.T. Paridah, Constr. Build. Mater. **106**, 149 (2016)
9. L. do Val Siqueira, C.I.L.F. Arias, B.C. Maniglia, C.C. Tadini, Curr. Opin. Food Sci.. Opin. Food Sci. **38**, 122 (2021)
10. F.M. AL-Oqla, J. Nat Fibre Polym. Compos. **1**, 1 (2022)
11. M. D. R. Islam, S. Ismail, J. Nat. Fibre Polym. Compos. **2**, 1 (2023)

12. J. Tarique, S.M. Sapuan, K. Abdan, R.A. Ilyas, E.S. Zainudin, S.F.K. Sherwani, and K.Z. Hazrati, Physical and barrier roperties of arrowroot (*Maranta Arundinacea*) starch based composites: a review, pp. 180–182, (2021)
13. M.Z. Asyraf, M.J. Suriani, C.M. Ruzaidi, A. Khalina, R.A. Ilyas, M.R.M. Asyraf, A. Syamsir, A. Azmi, A. Mohamed, Sustainability **14**, 7092 (2022)
14. J.P. Prakash, M.D. Anand, C.P. Jesuthanam, J.P. Pratheesh, and D.K.M.P, Int. J. Innov. Technol. Explor. Eng. *9*, 2462 (2019)
15. K. Murali Mohan Rao, K. Mohana Rao, A.V. Ratna Prasad, Mater. Des. **31**, 508 (2010)
16. M. Jawaid, S.S. Chee, M. Asim, N. Saba, S. Kalia, J. Clean. Prod. **330**, 129938 (2022)
17. P. Venkata Deepthi, K. Sita Raama Raju, M. Indra Reddy, Mater. Today Proc. **18**, 2114 (2019)
18. J. Liu, C. Jia, C. He, Proc. Soc Behav. Sci. **3**, 89 (2012)
19. A. Nurnadia, R.A. Roshafima, A.L.N. Shazwani, A. Hafizah, W.M.Z.W. Yunus, R. Fatehah, J. Nat. Fibre Polym. Compos. **2**, 1 (2023)
20. I. Yusuff, N. Sarifuddin, A.M. Ali, Prog. Rubber Plast. Recycl. Technol. **37**, 66 (2021)
21. S.M. Izwan, S.M. Sapuan, A.R. Mohamed, V.U. Siddiqui, J. Nat. Fibre Polym. Compos. **1**, 1 (2022)
22. M. Indra Reddy, U.R. Prasad Varma, I. Ajit Kumar, V. Manikanth, P.V. Kumar Raju, Mater. Today Proc. **5**, 5649 (2018)
23. M. N. M. Azlin, S. M. Sapuan, E. S. Zainudin, M. Y. M. Zuhri, and R. A. Ilyas, Natural Polylactic Acid-Based Fiber Composites: A Review, in *Advanced Processing, Properties, and Applications of Starch and Other Bio-Based Polymers*, Elsevier Inc. (2020), pp. 21–34. https://doi.org/10.1016/b978-0-12-819661-8.00003-2
24. H. Ku, H. Wang, N. Pattarachaiyakoop, M. Trada, Compos. Part B Eng. **42**, 856 (2011)
25. N.M. Nurazzi, K. Abdan, S.M. Sapuan, M.R.M. Asyraf, M.N.F. Norrrahim, K. Anton, J. Nat. Fibre Polym. Compos. **1**, 1 (2022)
26. M. F. M. Fauzi, M. R. M. Asyraf, S. A. Hassan, R. A. Ilyas, and T. Khan, J. Nat. Fibre Polym. Compos. **2**, 1 (2023)
27. J.J. Andrew, H.N. Dhakal, Compos. Part C Open Access **7**, 100220 (2022)
28. S.H. Sheikh Md Fadzullah, S.N.N. Ramli, Z. Mustafa, A.S. Razali, D. Sivakumar, I. Ismail, J. Adv. Manuf. Technol. **14**, 1 (2020)
29. E.S. Zainudin, H.A. Aisyah, N.M. Nurazzi, A. Kuzmin, J. Nat. Fibre Polym. Compos. **2**, 1 (2023)
30. S. Ramasamy, D. Jayabalakrishnan, and K. Thangappan, (2022). https://doi.org/10.37358/MP.22.2.5598
31. A.B.M. Supian, S.M. Sapuan, M. Jawaid, M.Y.M. Zuhri, R.A. Ilyas, A. Syamsir, Fibers Polym. **23**, 222 (2022)
32. A. Kumar Sharma, R. Bhandari, C. Sharma, S. Krishna Dhakad, C. Pinca-Bretotean, Mater. Today Proc. (2022). https://doi.org/10.1016/j.matpr.2021.12.592
33. S.M. Sapuan, Y. Nukman, The Relationship Between Manufacturing and Design for Manufacturing in Product Development of Natural Fibre Composites, in *Manufacturing of coir fiber reinforced polymer composites using hot compression technique*. (Springer, Selangor, 2014), p.2
34. A.G. Adeniyi, D.V. Onifade, J.O. Ighalo, A.S. Adeoye, Compos. Part B Eng. **176**, 107305 (2019)
35. Z.G. Mohammadsalih, M. Muawwidzah, V.U. Siddiqui, and S.M. Sapuan, J. Nat. Fibre Polym. Compos. **2**, 1 (2023)
36. D. Verma, P.C. Gope, The use of coir/coconut fibers as reinforcements in composites (2015). https://doi.org/10.1533/9781782421276.3.285
37. H.P.S.A. Khalil, M.S. Alwani, A.K.M. Omar, BioResources **1**, 220 (2006)
38. M.Z. Zainudin, M.R. Mansor, M.B. Ali, Y. Jameel, S.M. Sapuan, Basori, J. Nat. Fibre Polym. Compos. **2**, 1 (2023)
39. Y.S. Munde, R.B. Ingle, I. Siva, Adv. Mater. Process. Technol. **4**, 639 (2018)
40. P. Balakrishnan, M.J. John, L. Pothen, M.S. Sreekala, S. Thomas, Natural fibre and polymer matrix composites and their applications in aerospace engineering. Adv. Compos. Mater. Aerosp. Eng. (2016). https://doi.org/10.1016/b978-0-08-100037-3.00012-2
41. H. Danso, Proc. Eng. **200**, 1 (2017)
42. L. Yan, N. Chouw, L. Huang, B. Kasal, Constr. Build. Mater. **112**, 168 (2016)
43. C.A.S. Hill, H.P.S. Abdul Khalil, J. Appl. Polym. Sci.. Appl. Polym. Sci. **77**, 1322 (2000)
44. M.R.M. Asyraf, A. Syamsir, M.R. Ishak, S.M. Sapuan, N.M. Nurazzi, M.N.F. Norrrahim, R.A. Ilyas, T. Khan, M.Z.A. Rashid, Fibers Polym. **24**, 337 (2023)
45. A.L. Amir, M.R. Ishak, N. Yidris, M.Y.M. Zuhri, M.R.M. Asyraf, S.Z.S. Zakaria, Materials (Basel). **16**, 5021 (2023)
46. A.E. Hadi, J.P. Siregar, T. Cionita, A.P. Irawan, D.F. Fitriyana, R. Junid, J. Nat. Fibre Polym. Compos. **2**, 1 (2022)
47. M. Sharma, R. Sharma, S. Chandra Sharma, Mater. Today Proc. **46**, 6482 (2020)
48. M. Rafidah, M.R.M. Asyraf, N.M. Nurazzi, S.A. Hassan, R.A. Ilyas, T. Khan, W.A.A. Saad, A. Rashedi, S. Sharma, E.K. Hussein, Mater. Today Proc. (2023). https://doi.org/10.1016/j.matpr.2023.01.103
49. Q. Liu, M. Hughes, Compos. Part A Appl. Sci. Manuf. **39**, 1644 (2008)
50. C.V. Singh, R. Talreja, Int. J. Solids Struct.Struct. **45**, 4574 (2008)
51. M.K.R. Hashim, M.S.A. Majid, M.R.M. Jamir, F.H. Kasim, M.T.H. Sultan, Polymers (Basel). **13**, 1 (2021)
52. S.M. Bhasney, P. Bhagabati, A. Kumar, V. Katiyar, Compos. Sci. Technol. **171**, 54 (2019)
53. S.O. Ismail, E. Akpan, H.N. Dhakal, Compos. Part C Open Access **9**, 100322 (2022)
54. M.R.M. Asyraf, M.R. Ishak, D.D.C.V. Sheng, A.H.M. Hasni, A.L. Amir, M.F.A. Rased, M. Rafidah, M.N.F. Norrrahim, M.R. Razman, Z. Iskandar, Sustainability **15**, 10814 (2023)
55. M.H. Zin, K. Abdan, M.N. Norizan, The effect of different fiber loading on flexural and thermal properties of banana/pineapple leaf (PALF)/glass hybrid composite. Elsevier (2018). https://doi.org/10.1016/B978-0-08-102291-7.00001-0
56. J. Neto, H. Queiroz, R. Aguiar, R. Lima, D. Cavalcanti, M.D. Banea, J. Renew. Mater. **10**, 561 (2022)
57. M.R.M. Asyraf, A. Syamsir, N.M. Zahari, A.B.M. Supian, M.R. Ishak, S.M. Sapuan, S. Sharma, A. Rashedi, M.R. Razman, S.Z.S. Zakaria, R.A. Ilyas, M.Z.A. Rashid, Polymers (Basel). **14**, 920 (2022)
58. M.R.M. Asyraf, A. Syamsir, H. Bathich, Z. Itam, A.B.M. Supian, S. Norhisham, N.M. Nurazzi, T. Khan, M.Z.A. Rashid, Fibers Polym. **23**, 3232 (2022)
59. M.R. Ishak, S.M. Sapuan, Z. Leman, M.Z.A. Rahman, U.M.K. Anwar, J. Therm. Anal. Calorim.Calorim. **109**, 981 (2012)
60. M.G. Lomelí Ramírez, K.G. Satyanarayana, S. Iwakiri, G.B. De Muniz, V. Tanobe, T.S. Flores-Sahagun, Carbohydr. Polym. **86**, 1712 (2011)
61. R. Jumaidin, S.M. Sapuan, M. Jawaid, M.R. Ishak, J. Sahari, Int. J. Biol. Macromol.Macromol. **97**, 606 (2017)
62. M.R.M. Huzaifah, S.M. Sapuan, Z. Leman, M.R. Ishakc, BioResources **14**, 619 (2019)
63. A. Nazrin, S.M. Sapuan, M.Y.M. Zuhri, Polymers (Basel). **12**, 1 (2020)
64. A.M. Radzi, S.M. Sapuan, M. Jawaid, M.R. Mansor, J. Mater. Res. Technol. **8**, 3988 (2019)
65. J.T. Kim, A.N. Netravali, Compos. Part A Appl. Sci. Manuf. **41**, 1245 (2010)

66. F.H. Abdalla, S.A. Mutasher, Y.A. Khalid, S.M. Sapuan, A.M.S. Hamouda, B.B. Sahari, M.M. Hamdan, Mater. Des. **28**, 234 (2007)
67. V.P. Arthanarieswaran, A. Kumaravel, M. Kathirselvam, Mater. Des. **64**, 194 (2014)
68. F. Yang, H. Long, B. Xie, W. Zhou, Y. Luo, C. Zhang, X. Dong, J. Appl. Polym. Sci.Polym. Sci. **137**, 1 (2020)
69. L.F. Ng, M.Y. Yahya, Z. Mustafa, Polym. Compos. **43**, 6667 (2022)
70. G.A. Dress, M.H. Woldemariam, D.T. Redda, Adv. Mater. Sci. Eng. **2021**, 6669600 (2021)
71. A.M.R. Azmi, M.T.H. Sultan, M. Jawaid, A.F.M. Nor, A newly developed bulletproof vest using kenaf-X-ray film hybrid composites, in *Mechanical and Physical Testing of Biocomposites, Fibre-Reinforced Composites and Hybrid Composites*. ed. by M. Jawaid, M.T.H. Sultan (Woodhead Publishing, S. N. Amsterdam, 2018), pp.157–169. https://doi.org/10.1016/B978-0-08-102292-4.00009-6